

## Theory of magnetoelectric effects at magnetoacoustic resonance in single-crystal ferromagnetic-ferroelectric heterostructures

M. I. Bichurin, V. M. Petrov, O. V. Ryabkov, and S. V. Averkin

*Department of Engineering Physics, Novgorod State University, B. S. Peterburgskaya St. 41, 173003 Veliky Novgorod, Russia*

G. Srinivasan

*Physics Department, Oakland University, Rochester, Michigan 48309, USA*

(Received 16 April 2005; published 29 August 2005)

A theoretical model that predicts very strong magnetoelectric (ME) interactions at magnetoacoustic resonance (MAR) in single-crystal ferrite-piezoelectric bilayer is discussed. In such bilayers, the ME interactions are mediated by mechanical strain. We considered ME coupling at the coincidence of electromechanical resonance for the electrical subsystem and ferromagnetic resonance for the ferrite. The theory predicts efficient transfer of energy between phonons, spin waves, and electric and magnetic fields at MAR. Ultrahigh ME coefficients, on the order of 80–480 V/cm Oe at 5–10 GHz, are expected for nickel ferrite-lead zirconate titanate (PZT) and yttrium-iron garnet-PZT bilayers. The phenomenon is also of importance for the realization of multifunctional ME nanosensors/transducers operating at microwave frequencies.

DOI: [10.1103/PhysRevB.72.060408](https://doi.org/10.1103/PhysRevB.72.060408)

PACS number(s): 75.80.+q, 76.50.+g, 72.55.+s, 77.65.-j

Materials that are magnetoelectric show an induced polarization (magnetization) in an applied magnetic (electric) field. Layered ferromagnetic-ferroelectric heterostructures have attracted considerable attention in this regard due to the observation of giant magnetoelectric (ME) effects that is facilitated by the sample response to electric, magnetic, and elastic forces.<sup>1</sup> Composites consisting of magnetostrictive ferrites, manganites, or terfenol with piezoelectric lead zirconate titanate (PZT) or lead magnesium niobate-lead titanate (PMN-PT), are found to show strong ME coupling.<sup>2–6</sup> Such heterostructures also provide us with unique opportunities for theoretical and experimental studies on ME coupling when the magnetic and/or electric subsystems show resonance behavior. Two types of resonances are of importance: electromechanical resonance (EMR) for the piezoelectric component and ferromagnetic resonance (FMR) for the magnetic phase.<sup>7–12</sup> This work focuses on ME interaction at the coincidence of EMR and FMR, i.e., magnetoacoustic resonance (MAR).

Consider first the ME interactions at EMR that give rise to the following phenomena:

(i) A shift  $\delta f_r$  in the EMR frequency  $f_r$  in a static magnetic field  $H$  due to changes in the composite's Young's modulus ( $\delta E$  effect). We developed a theoretical model for the effect and observed the predicted frequency shift in several systems. Our studies show that the ratio  $\delta f_r/H$  is a sensitive measure of the strength of ME coupling.<sup>12</sup>

(ii) A resonant enhancement in the ME susceptibility  $\alpha = \delta P / \delta H$  when the ac magnetic field  $\delta H$  is tuned to EMR. The ME coupling at EMR is similar in nature to the low-frequency coupling, i.e., an induced polarization  $\delta P$  under the action of  $\delta H$ . But  $\delta H$  is tuned to the frequency for radial or thickness acoustic modes. Several composites, including ferrite-PZT, terfenol-D with PZT or PVDF, and ferromagnetic transition metal/alloy-PZT, systems, show the expected resonant coupling and the results are in good agreement with theoretical predictions.<sup>11,13,14</sup>

One expects similar phenomena at resonance for the magnetic subsystem, i.e., electric-field effects on the ferromagnetic resonance field and a resonant enhancement in ME coupling. Our earlier theoretical models predicted an electric field  $E$  to cause a shift  $\delta H_r$  in the resonance field.<sup>8,9</sup> We did observe this shift in systems including lithium ferrite-PZT and single-crystal yttrium-iron garnet (YIG)/lead magnesium niobate-lead titanate (PMN-PT). Theoretical estimates of ME coupling parameter  $A = \delta H_r/E$  were found to be in good agreement with data.<sup>10</sup>

Here we provide a theory for ME interactions at the coincidence of FMR and EMR, at magnetoacoustic resonance. At FMR, spin-lattice coupling and spin waves that couple energy to phonons through relaxation processes are expected to enhance the piezoelectric and ME interactions. Further strengthening of ME coupling is expected at the overlap of FMR and EMR. A past effort of significance in this regard is the work by Tilley and Scott on theoretical estimates of magnetoelectric susceptibilities in  $\text{BaMnF}_4$  under high-frequency magnetic excitations and phonons.<sup>15</sup>

Here we consider ME interactions under magnetoacoustic resonance in ferrite-PZT bilayers with low-loss ferrites such as nickel ferrite or YIG that would facilitate observation of the effects predicted in this work. Significant results and implications of our present work are as follows: (i) Coincidence of FMR and EMR allows energy transfer between phonons, spin waves, and electric and magnetic fields. This transfer is found to be very efficient in ferrite-PZT. (ii) Ultrastrong ME interactions are predicted at magnetoacoustic resonance with ME voltage coefficients on the order of several hundred V/cm Oe. (iii) The work is also of technological importance. The ME effect at MAR can be utilized for the realization of miniature and/or nanosensors and transducers operating at high frequencies since the coincidence is predicted to occur at microwave frequencies in the bilayers.

We consider a ferrite-PZT bilayer as in Fig. 1 that is subject to a bias field  $H_0$  perpendicular to its plane. The piezo-

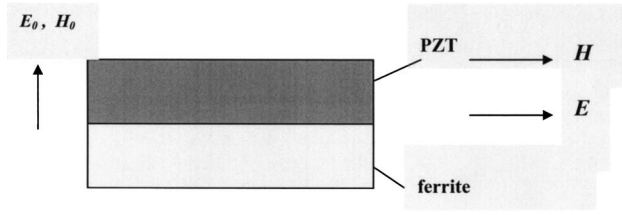


FIG. 1. A bilayer of ferrite and PZT.  $H_0$  is the dc bias field,  $H$  and  $E$  are microwave magnetic and electric fields. Electric poling field  $E_0$  is along  $H_0$ .

electric phase is assumed to be electrically polarized with a field  $E_0$  parallel to  $H_0$  and that  $H_0$  is high enough to drive the ferrite to a saturated (single-domain) state that has two advantages. When domains are absent, acoustic losses are minimum. The single-domain state under FMR provides the conditions necessary for achieving a large effective susceptibility.

The free-energy density of the ferrite is given by

$${}^m W = W_H + W_{an} + W_{ma} + W_{ac}, \quad (1)$$

where  $W_H = -\mathbf{M} \times \mathbf{H}_i$  is the Zeeman energy,  $\mathbf{M}$  is the magnetization, and  $H_i$  is the internal magnetic field that includes demagnetizing fields. The term  $W_{an}$ , given by

$$W_{an} = K_1/M_0^4(M_1^2 M_2^2 + M_2^2 M_3^2 + M_3^2 M_1^2),$$

is the cubic crystalline anisotropy energy with  $K_1$  the cubic anisotropy constant and  $M_0$  the saturation magnetization. The magnetoelastic energy is written as

$$W_{ma} = B_1/M_0^2(M_1^{2m} S_1 + M_2^{2m} S_2 + M_3^{2m} S_3) + B_2/M_0^2(M_1 M_2^m S_6 + M_2 M_3^m S_4 + M_1 M_3^m S_5),$$

where  $B_1$  and  $B_2$  are magnetoelastic coefficients and  $S_i$  are the elastic strains. Finally, the elastic energy is

$$W_{ac} = \frac{1}{2} {}^m c_{11} ({}^m S_1^2 + {}^m S_2^2 + {}^m S_3^2) + \frac{1}{2} {}^m c_{44} ({}^m S_4^2 + {}^m S_5^2 + {}^m S_6^2) + {}^m c_{12} ({}^m S_1 {}^m S_2 + {}^m S_2 {}^m S_3 + {}^m S_1 {}^m S_3)$$

and  ${}^m c_{ij}$  are moduli of elasticity.

The generalized Hooke's law for the piezoelectric phase can be presented as<sup>16</sup>

$$\begin{aligned} {}^p T_4 &= {}^p c_{44} {}^p S_4 - {}^p e_{15} {}^p E_2, \\ {}^p T_5 &= {}^p c_{44} {}^p S_5 - {}^p e_{15} {}^p E_1, \end{aligned} \quad (2)$$

where  $e_{p15}$  is the piezoelectric coefficient and  ${}^p E$  is the electric field. Equations of motion for the ferrite and piezoelectric phases can be written in the following form:

$$\begin{aligned} \partial^2 ({}^m u_1) / \partial t^2 &= \partial^2 ({}^m W) / (\partial x \partial^m S_1) + \partial^2 ({}^m W) / (\partial y \partial^m S_6) \\ &+ \partial^2 ({}^m W) / (\partial z \partial^m S_5), \end{aligned}$$

$$\begin{aligned} \partial^2 ({}^m u_2) / \partial t^2 &= \partial^2 ({}^m W) / (\partial x \partial^m S_6) + \partial^2 ({}^m W) / (\partial y \partial^m S_2) \\ &+ \partial^2 ({}^m W) / (\partial z \partial^m S_4), \end{aligned}$$

$$\partial^2 ({}^p u_1) / \partial t^2 = \partial ({}^m T_1) / \partial x + \partial ({}^m T_6) / \partial y + \partial ({}^m T_5) / \partial z,$$

$$\partial^2 ({}^p u_2) / \partial t^2 = \partial ({}^m T_6) / \partial x + \partial ({}^m T_2) / \partial y + \partial ({}^m T_4) / \partial z. \quad (3)$$

The equation of motion of magnetization for the ferrite has the form

$$\partial \mathbf{M} / \partial t = -\gamma [\mathbf{M}, \mathbf{H}_{\text{eff}}], \quad (4)$$

where  $\mathbf{H}_{\text{eff}} = -\partial ({}^m W) / \partial \mathbf{M}$ .

Next we consider waves with circular components by introducing

$$\begin{aligned} m^+ &= m_1 + im_2, \\ H^+ &= H_{1+} + iH_{2+}, \\ E^+ &= E_{1+} + iE_{2+}, \\ u^+ &= u_{1+} + iu_{2+}, \end{aligned} \quad (5)$$

where  $m$  is the ac magnetization and  $u$  is the displacement. Equations (2)–(4) can be transformed to the following form for harmonic waves propagating in the  $z$  direction:

$$\begin{aligned} \omega m^+ &= \gamma [H_0 m^+ + B_2 \partial ({}^m u^+) / \partial z - 4\pi M_0 m^+ - M_0 H^+], \\ -\omega^2 m^+ \rho^m u^+ &= {}^m c_{44} \partial^2 ({}^m u^+) / \partial z^2 + (B_2 / M_0) \partial ({}^m m^+) / \partial z, \\ -\omega^2 \rho^p u^+ &= {}^p c_{44} \partial^2 ({}^p u^+) / \partial z^2, \end{aligned} \quad (6)$$

where  $\omega$  is the angular frequency and  ${}^m \rho$  and  ${}^p \rho$  are densities of ferrite and piezoelectric layers.

The equation of motion for the ferrite layer can be simplified when we assume  $H$  to be homogeneous in the sample volume. Taking into consideration spatially alternating magnetization induced contributions, we obtain

$$-\omega^2 {}^m \rho^m u^+ = {}^m c_{44}^+ \partial^2 ({}^m u^+) / \partial z^2, \quad (7)$$

with the effective modulus of elasticity  ${}^m c_{44}^+$  given by

$${}^m c_{44}^+ = {}^m c_{44} + \gamma B_2^2 / [M_0 (\omega - \gamma H_0 + \gamma 4\pi M_0)]. \quad (8)$$

Boundary conditions at the interface and at the top and bottom bilayer surfaces may be written as

$${}^m u^+ = {}^p u^+ \text{ at } z = 0;$$

$${}^m c_{44}^+ \partial ({}^m u^+) / \partial z + B_2 m_0^+ / M_0 = 0 \text{ at } z = {}^m L;$$

$${}^m c_{44}^+ \partial ({}^m u^+) / \partial z + B_2 m_0^+ / M_0 = {}^p c_{44} \partial ({}^p u^+) / \partial z - {}^p e_{15} {}^p E^+ \text{ at } z = 0;$$

$${}^p c_{44} \partial ({}^p u^+) / \partial z - {}^p e_{15} {}^p E^+ = 0 \text{ at } z = -{}^p L, \quad (9)$$

where  ${}^m L$  and  ${}^p L$  are ferrite and piezoelectric layer thicknesses, and

$$m_0^+ = -\gamma M_0 / (\omega - \gamma H_0 + \gamma 4\pi M_0)$$

is the homogeneous ac magnetization in sample volume. It is clear from Eq. (9) that the mechanical displacement and the FMR uniform precession mode for the ferrite are related through boundary conditions at the interface. The induced electric field in PZT,  $E^+$ , can be found using the open circuit condition

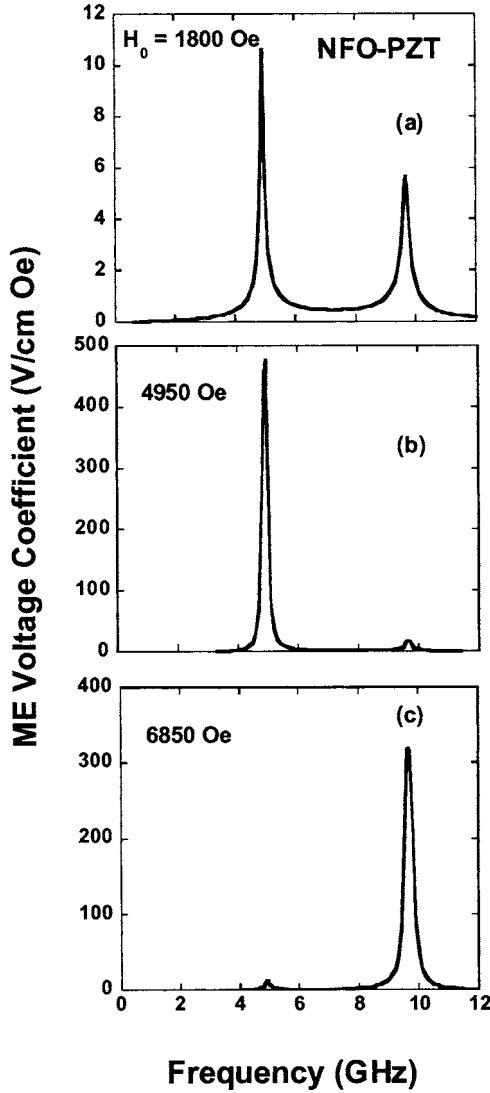


FIG. 2. Theoretical estimates on the variation of magnetoelectric (ME) voltage coefficient  $\alpha_E$  with the frequency of ac magnetic field for a bilayer, as in Fig. 1, of nickel ferrite (NFO)-lead zirconate titanate (PZT). The thickness of NFO and PZT layers are 100 and 200 nm, respectively. (a) The bias field  $H_0$  is smaller than the field  $H_r$  for ferromagnetic resonance (FMR) in NFO. The peaks in  $\alpha_E$  occur at the fundamental and second harmonic in electromechanical resonance (EMR) for thickness modes for the bilayer. (b) The ME coupling at the coincidence of EMR and FMR, the magnetoacoustic resonance (MAR).  $H_0$  is selected so that FMR in NFO coincides with the fundamental EMR mode, resulting in the enhancement in  $\alpha_E$  at MAR. (c) Similar result as in (b), but for MAR at the second harmonic of acoustic modes in NFO-PZT.

$$D^+ = \frac{1}{pL} \int_{-pL}^0 {}^pD^+ dz = 0, \quad (10)$$

where  ${}^pD^+ = {}^pe_{15}{}^pS^+ + {}^p\varepsilon_{11}{}^pE^+$  is the electric displacement and  ${}^p\varepsilon_{11}$  is the permittivity of the piezoelectric component at constant strain. Substituting the solutions of Eq. (6) in Eq. (10), and taking into account Eqs. (2) and (9), one obtains the following expression for the ME voltage coefficient:

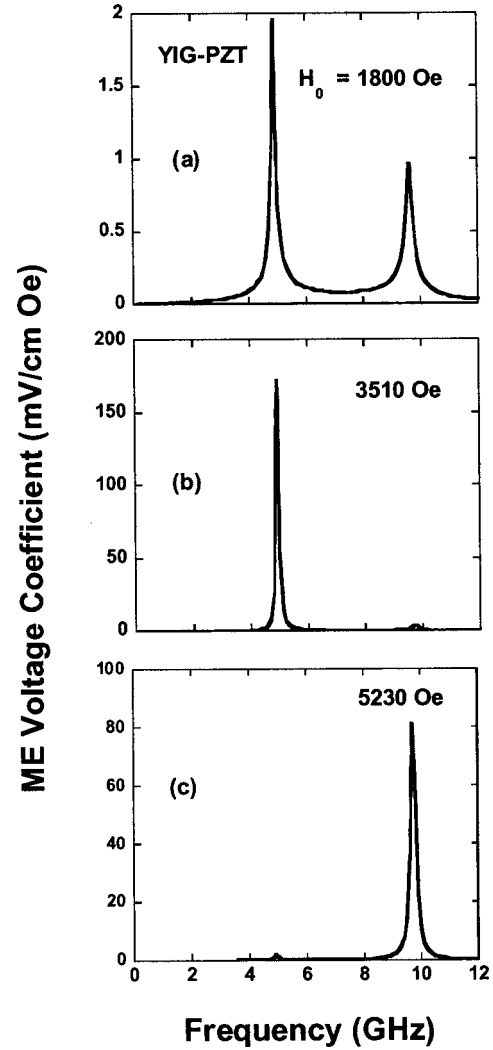


FIG. 3. Results as in Fig. 2 for a bilayer of yttrium-iron garnet (YIG) and PZT.

$$\begin{aligned} |E^+/H^+| = & \gamma B_2 {}^pc_{44} {}^pk {}^pe_{15} [1 - \cos({}^pk {}^pL)] [1 - \cos({}^mk {}^mL)] / \{ [\omega \\ & - \gamma H_0 + 4\pi\gamma M_0] [{}^pk {}^pc_{44} \cos({}^mk {}^mL)] (2{}^pe_{15}^2) \\ & \times [1 - \cos({}^pk {}^pL) + \sin({}^pk {}^pL) {}^pc_{44} {}^p\varepsilon_{11} {}^pk {}^pL] \\ & + {}^mk {}^mc_{44}^+ \sin({}^mk {}^mL) ({}^pe_{15}^2 \sin({}^pk {}^pL) \\ & + \cos({}^pk {}^pL) {}^pc_{44} {}^p\varepsilon_{11} {}^pk {}^pL] \}, \quad (11) \end{aligned}$$

where  ${}^mk = \omega \sqrt{{}^m\rho / {}^mc_{44}^+}$ ,  ${}^pk = \omega \sqrt{{}^p\rho / {}^pc_{44}}$ .

The model allows the estimation of the ME voltage coefficient in a bilayer as a function of frequency of ac magnetic field. Now we apply the theory to two specific bilayer systems: (i) nickel ferrite (NFO)-PZT and (ii) YIG-PZT. Both NFO and YIG have low losses at FMR, a necessary condition for the observation of the enhancement in ME coupling at MAR. We need to consider only the thickness EMR modes because radial modes will not couple to FMR due to field polarization considerations. One must also assume appropriate thicknesses for the ferrite and PZT so that EMR occurs at a frequency for which FMR is realized for a magnetically

saturated state in the ferrite, around 3–5 GHz for YIG and NFO.

First we consider a bilayer of NFO-PZT. Figure 2 shows the theoretical ME voltage coefficient  $\alpha_E$  versus frequency for (i) a bias field  $H_0$  that is much smaller than the FMR resonance field  $H_r$  and (ii)  $H_0$  set at FMR. For  $H_0 < H_r$ , Fig. 2(a) shows peaks in the ME voltage coefficient at the fundamental and higher harmonic EMR. The static magnetic field for FMR,  $H_r$ , is given by

$$H_r = \omega/\gamma - 4\pi M_0.$$

As  $H_0$  is increased to  $H_r$ ,  $\alpha_E$  is expected to show a dramatic increase in magnitude due to a resonancelike character for the mechanical displacement in the FMR region [Eq. (11)]. Figure 2 shows the estimated  $\alpha_E$  versus  $f$  for  $H_0 = H_r$  at the fundamental or second harmonic. Signal attenuation is taken into account in these calculations by introducing a complex frequency with an imaginary component of  $10^7$  rad/s. Figure 2(b) shows  $\alpha_E$  versus  $f$  for the specific case in which MAR occurs at the fundamental EMR mode; one anticipates a 40-fold increase in  $\alpha_E$  from low-field values to 480 V/cm Oe for  $H_0 = H_r$  at MAR. Similar results at the second harmonics are shown in Fig. 2(c) and the relative enhancement in  $\alpha_E$  is higher for this mode than for the fundamental.

Similar estimates of  $\alpha_E$  versus  $f$  are shown in Fig. 3 for YIG-PZT. The anticipated enhancement in  $\alpha_E$  at EMR is higher in YIG-PZT than for NFO-PZT. The most significant inferences from the theory and estimates of  $\alpha_E$  versus  $f$  in Figs. 2 and 3 are as follows:

(i) The parameters that determine the MAR frequencies are the layer thicknesses and the bias magnetic field, and

must fulfill the conditions for EMR and FMR, respectively. The MAR frequency can easily be controlled by choosing bilayer materials with desired parameters, layer thickness, and the bias field. It is possible to move to a higher MAR frequency by choosing higher-order EMR. One may also select a higher MAR frequency by just reducing the layer thickness. For example, MAR is expected to occur at 2.5, 5, and 10 GHz in nanobilayers of thicknesses 200, 100, and 50 nm, respectively. But the bilayer diameter must be 10–20 times the thickness in order to reduce the demagnetization fields.

(ii) A giant ME voltage coefficient results from overlap of the FMR and EMR at the fundamental or higher harmonics.

(iii) The magnitude of  $\alpha_E$  at EMR and MAR are higher in NFO-PZT than for YIG-PZT due to strong magnetoelastic interaction (coefficient  $B_2$ ) for NFO.

In conclusion, a theoretical model has been developed for ME effects in a single-crystal ferrite-piezoelectric bilayer in the magnetoelastic resonance region. The theory predicts a giant ME effect at MAR. The enhancement arises from interaction between elastic modes and the uniform precession spin-wave mode, resulting in magnetoelastic modes. The peak ME voltage coefficient appears at the coincidence of acoustic resonance and FMR frequencies. Estimates for nominal bilayer parameters for nickel ferrite-PZT and YIG-PZT predict MAR at 5–10 GHz and ME voltage coefficients on the order of 80–480 V/cm Oe.

The work at Oakland University was supported by grants from the National Science Foundation (DMR-0302254), the Army Research Office (W911NF-04-1-0299), and the Office of Naval Research (N00014-05-1-0664).

<sup>1</sup>Hans Schmid, in *Introduction to Complex Mediums for Optics and Electromagnetics*, edited by W. S. Weiglhofer and A. Lakhtakia (SPIE, Bellingham, WA, 2003), p. 167.

<sup>2</sup>T. G. Lupeiko, I. V. Lisnevskaya, M. D. Chkheidze, and B. I. Zvyagintsev, *Inorg. Mater.* **31**, 1245 (1995).

<sup>3</sup>G. Srinivasan, E. T. Rasmussen, J. Gallegos, R. Srinivasan, Yu. I. Bokhan, and V. M. Laletin, *Phys. Rev. B* **64**, 214408 (2001).

<sup>4</sup>K. Mori and M. Wuttig, *Appl. Phys. Lett.* **81**, 100 (2002).

<sup>5</sup>J. G. Wan, J.-M. Liu, H. L. W. Chand, C. L. Choy, G. H. Wang, and C. W. Nan, *J. Appl. Phys.* **93**, 9916 (2003).

<sup>6</sup>S. Dong, J. F. Li, and D. Viehland, *Philos. Mag. Lett.* **83**, 769 (2003); *IEEE Trans. Ultrason. Ferroelectr. Freq. Control* **50**, 10 (2003).

<sup>7</sup>M. I. Bichurin, D. A. Filippov, V. M. Petrov, and G. Srinivasan, *Proceedings of the International Conference on the Physics of Electronic Materials*, Kaluga, Russia, 2002 (unpublished).

<sup>8</sup>M. I. Bichurin, I. A. Kornev, V. M. Petrov, A. S. Tatarenko, Yu. V. Kiliba, and G. Srinivasan, *Phys. Rev. B* **64**, 094409 (2001).

<sup>9</sup>M. I. Bichurin, V. M. Petrov, Yu. V. Kiliba, and G. Srinivasan, *Phys. Rev. B* **66**, 134404 (2002).

<sup>10</sup>S. Shastry, G. Srinivasan, M. I. Bichurin, V. M. Petrov, and A. S. Tatarenko, *Phys. Rev. B* **70**, 064416 (2004).

<sup>11</sup>M. I. Bichurin, D. A. Filippov, V. M. Petrov, V. M. Laletin, N. Paddubnaya, and G. Srinivasan, *Phys. Rev. B* **68**, 132408 (2003).

<sup>12</sup>G. Srinivasan, C. P. De Vreugd, V. M. Laletin, N. Paddubnaya, M. I. Bichurin, V. M. Petrov, and D. A. Filippov, *Phys. Rev. B* **71**, 184423 (2005).

<sup>13</sup>N. Cai, J. Zhai, C. W. Nan, Y. Lin, and Z. Shi, *Phys. Rev. B* **68**, 224103 (2003).

<sup>14</sup>S. Dong, J. Cheng, J. F. Li, and D. Viehland, *Appl. Phys. Lett.* **83**, 4812 (2003).

<sup>15</sup>D. R. Tilley and J. F. Scott, *Phys. Rev. B* **25**, 3251 (1982).

<sup>16</sup>*Physical Acoustics*, edited by W. P. Mason (Academic, New York and London, 1965), Vol. III, Part B.